Spray Forming of Bulk Ultrafine-Grained Al-Fe-Cr-Ti

C. BANJONGPRASERT, S.C. HOGG, E. LIOTTI, C.A. KIRK, S.P. THOMPSON, J. MI, and P.S. GRANT

An Al-2.7Fe-1.9Cr-1.8Ti alloy has been spray formed in bulk and the microstructure and properties compared with those of similar alloys produced by casting, powder aomization (PA), and mechanical alloying (MA) routes. In PA and MA routes, a nanoscale metastable icosahedral phase is usually formed and is known to confer high tensile strength. Unlike previous studies of the spray forming of similar Al-based metastable phase containing alloys that were restricted to small billets with high porosity, standard spray forming conditions were used here to produce a ~98 pct dense 19-kg billet that was hot isostatically pressed (''HIPed''), forged, and/or extruded. The microstructure has been investigated at all stages of processing using scanning electron microscopy (SEM), electron backscatter diffraction (EBSD), and synchrotron X-ray diffraction (XRD) at the Diamond Light Source. Consistent with the relatively low cooling rate in spray forming under standard conditions, the microstructure showed no compelling evidence for the formation of metastable icosahedral phases. Nonetheless, after downstream processing, the spray-formed mechanical properties as a function of temperature were very similar to both PA rapid solidification (RS) materials and those made by MA. These aspects have been rationalized in terms of the typical phases, defects, and residual strains produced in each process route.

DOI: 10.1007/s11661-010-0386-0

I. INTRODUCTION

BULK metastable/nanostructured Al alloys are suggested to provide a step change in the properties of Al alloys by the virtue of a large fraction of hard and shear-resistant fine scale metastable particles, grain size strengthening effects, extended solid solubility strengthening, and even amorphous phase formation in which dislocation motion is highly restricted. It is also widely acknowledged that in order for these materials to realize their full potential, new combinations of composition and process route must be developed in order to produce genuine bulk materials cost-effectively, while avoiding some of the common disadvantages such as limited toughness. Despite steady progress, the exciting properties provided by extreme microstructural refinement and significant deviation from thermodynamic equilibrium are still generally only achievable through rapid solidification (RS) and mechanical alloying (MA) processes of small volumes of alloy that must be reconstituted back to bulk at elevated temperature, usually with an accompanying degradation of properties.

Recently, there have been feasibility studies of producing nanostructured alloys in bulk by spray forming. Although cooling rates in the spray phase of spray forming can be comparatively high, residual solidification in the billet phase is much slower, as is solid-state cooling. Afonso *et al.*[1,2] investigated the spray forming of Al-Y-Ni-Co-(Zr) alloys, producing ~7-kg billets of $Al_{85}Y_8Ni_5Co_2$ and a 2.1-kg billet of $Al_{84}Y_3Ni_8Co_4Zr_1$ (at. pct). Using a relatively high gas to metal mass flow ratio to enhance the cooling rate, billets contained up to ~76 vol pct of an amorphous Al-rich phase but suffered from high porosity because of insufficient liquid feeding on the billet top surface. Al-RE-TM (RE = rare earth, TM = transition metal) alloys were spray formed by Guo *et al.*[3–5] A spray-formed 1-kg, 230-mm-diameter, and 3-mm-thick plate of $Al_{89}La_6Ni_5$ had ~36 vol pct of an Al-rich phase; while a 2-kg, 230-mm-diameter, and 30-mm-thick plate of $Al_{85}Nd_5Ni_{10}$ alloy contained ~63 vol pct amorphous Al-rich phase.

While it has been shown that spray forming of complex composition alloys that form glasses or nanostructured materials in powders or ribbons is feasible, so far this has only been possible where low porosity and homogeneity were sacrificed and, by modern spray forming standards, very small deposits were manufactured. In other words, some of the inherent benefits of spray forming such as large scale processing of homogeneous low defect material have been sacrificed in pursuit of strong departures from equilibrium. In this article, we present a study of a 19-kg nominally Al-3Fe-2Cr-2Ti (at. pct) billet produced under standard spray forming conditions. We assess to what extent the

C. BANJONGPRASERT, formerly Research Student, Department of Materials, Oxford University, is Lecturer, Faculty of Science, Chiang Mai University, Chiang Mai 50200, Thailand. J. MI, Research Assistant, and P.S. GRANT, Cookson Chair of Materials, are with the Department of Materials, Oxford University, Oxford OX1 3PH, United Kingdom. Contact e-mail: patrick.grant@materials.ox.ac.uk S.C. HOGG, Lecturer, and E. LIOTTI, Research Student, Department of Materials, and C.A. KIRK, Lecturer, Department of Chemistry, are with Loughborough University, Loughborough, LE11 3TU, United Kingdom. S.P. THOMPSON, Beamline Scientist, is with Diamond Light Source, Harwell Science and Innovation Campus, Didcot, Oxfordshire OX11 0DE, United Kingdom.

Manuscript submitted November 23, 2009.
Article published online August 13, 2010

"conventional" RS (10^3 to 10^5 K/s) microstructure of this alloy is compromised by the slower average cooling rate in spray forming (10^1 to 10^3 K/s), and whether the resultant mechanical properties—available in bulk—offer encouragement for the spray forming of this class of alloy. Al-3Fe-2Cr-2Ti provides a useful benchmark alloy since it has been produced elsewhere by suction casting,[6] RS of powders followed by consolidation,[7–9] and MA of powders followed by consolidation.[10–12]

II. EXPERIMENTAL

The nominal composition alloy Al-3Fe-2Cr-2Ti (at. pct) was vacuum induction melted from master alloys, solidified, inverted, and then remelted under Ar for spray forming using the Sandvik–Osprey plant installed at Oxford University with process conditions described elsewhere[13] to produce a 19-kg billet. The composition of the as-spray-formed alloy was measured by inductively coupled plasma–optical emission spectroscopy at London & Scandinavian Metallurgical Co. Ltd. (Rotherham, UK) at the billet midheight midradius as Al-2.7Fe-1.9Cr-1.8Ti (at. pct). Traces of Zr and Si arose because of interactions of the high-temperature melt at ~1723 K (~1500 °C) with refractories and the zirconia pouring nozzle. Some deviation from the target composition also occurred due to evaporation/slag formation (removed before spraying) at the very high melt temperatures required.

As-spray-formed material was hot isostatically pressed ("HIPed") at either 723 K (450 °C), 4 hours at 100 MPa or 823 K (550 °C) for 2 hours at 190 MPa. The 823 K (450 °C) HIPed material was then either hot forged at 673 K (400 °C) to a true strain of 1 or extruded at 748 K (475 °C) to 7.5-mm bar at an extrusion ratio of 16:1. Tensile testing of HIPed and forged materials was performed according to ASTM E8 at room temperature and ASTM E21 at elevated temperatures up to 673 K (400 °C).

The microstructure of the billet in various conditions was investigated using scanning electron microscopy (SEM) and electron backscatter diffraction (EBSD) in a JEOL* JSM 6500F, a LEO VP1530, and an FEI NOVA 600 Nanolab operating in low voltage, backscattered electron imaging mode, which provided strong crystallographic orientation contrast. Synchrotron X-ray diffraction (XRD) was performed using the I11 high-resolution powder diffraction beamline at the Diamond Light Source.[14] The radiation wavelength was 0.826027 Å. High-resolution diffraction data were collected *via* five multianalyzer crystal stages, equipped with Si 111 analyzer crystals. The X-ray data were analyzed using Topas-academic V4.1 software (Brisbane, Australia) to estimate the possible separate contributions of both diffracting crystallite size effects and residual strain to any α-Al peak broadening.[15] Because of the very high instrument resolution provided by I11 at Diamond, peak broadening due to crystallite size and residual strain effects could be determined over wider ranges and with greater sensitivity than achievable in laboratory-based XRD. Prior to experiments, the measured crystallite size of a certified NIST SRM660a LaB_6 standard was determined by peak broadening analysis to be 2.14 μm, which was in excellent agreement with the certified domain size of 2 μm. Consequently, any underlying contributions due to instrument broadening effects were removed, and peak broadening effects due to grain size were calibrated for sizes up to ~2 μm. Pawley structureless whole pattern fitting of the XRD data was also performed using the modified Thompson-Cox-Hasting pseudo-Voight profile function.[14]

*JEOL is a trademark of Japan Electron Optics Ltd., Tokyo.

III. RESULTS AND DISCUSSION

A. *Spray-Formed Material*

Figure 1 shows the billet base contained macropore defects due to initial process instability, while the rest of the billet was free of macrodefects, containing 2 to 3 area pct porosity typical of spray-formed material and generally lower than previously spray-formed amorphous and nanostructured alloy compositions from the literature.[1–5] However, when compared with the usual high microstructural homogeneity of spray-formed conventional Al alloys,[16] the microstructure was inhomogeneous, as shown in the unetched microstructure in

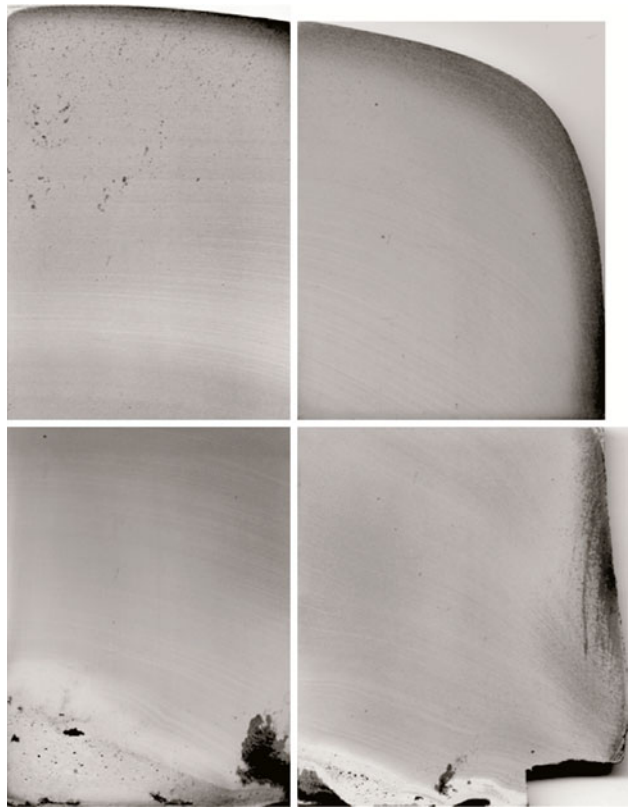

Fig. 1—Quarter cross section of the spray-formed Al-2.7Fe-1.9Cr-1.8Ti billet.

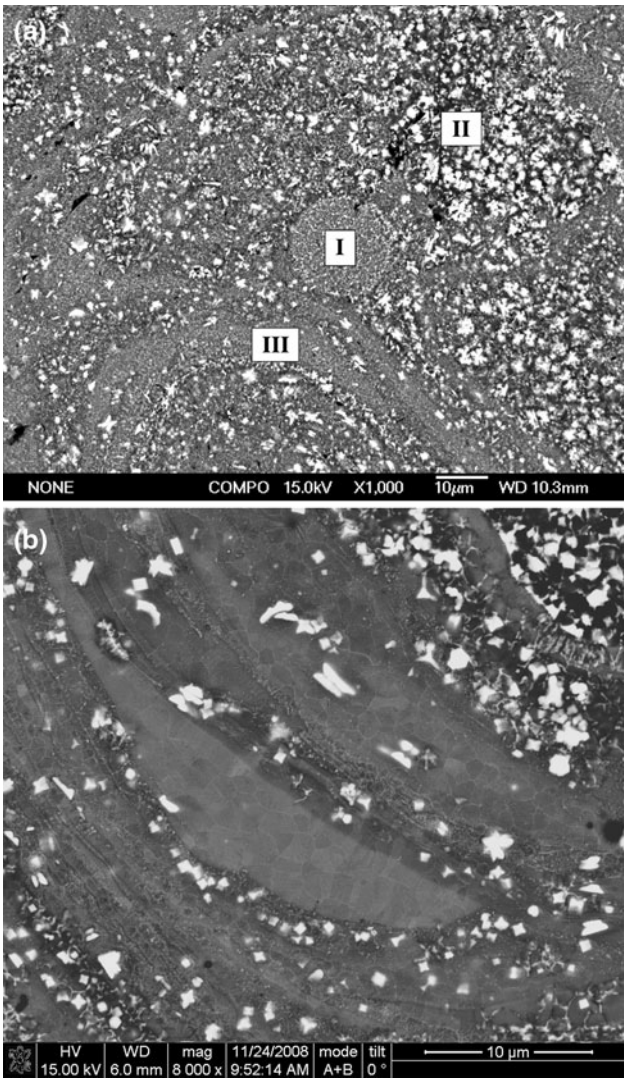

Fig. 2—Backscattered electron images of as-spray-formed Al-Fe-Cr-Ti illustrating microstructural heterogeneity: (*a*) three regions: (I) presolidified droplet, (II) fine particles, and (III) ultrafine particles; and (*b*) high magnification of a region III type structure, showing very fine submicron particles and micron-sized α-Al grains.

Figure 2. There was a high intermetallic second-phase particle fraction, approaching 50 pct in some regions, within an overall complex and fine-scale microstructure. The microstructure comprised three regions: (I) near spherical presolidified droplets containing submicron particles; (II) micron-sized particles within swirls originating from relatively large liquid droplets (ca. >100 μm) that then deformed into ''splats'' with widths of a few tens of microns, and (III) ultrafine submicron particles in thin splats with widths of microns. Within some of the regions, there were α-Al grains of diameter <1 μm, as shown by the good grain orientation contrast in Figure 2(b). The heterogeneity of the spray-formed microstructure was similar to the same alloy produced by suction casting in Reference 6 at cooling rates similar to spray forming, but the as-spray-formed microstructure was typically 3 to 4 times finer.[6]

In conventional, lower melting point Al alloys, the spray-formed microstructure is generally more homogeneous than the Al-Fe-Cr-Ti alloy here because of the large amount of solid remelting at deposition.[16] In Al-Fe-Cr-Ti, many of the intermetallic particles form comparatively early in the solidification path, at high temperature, by peritectic or pseudo-peritectic reactions in the atomized droplets and at comparatively high cooling rate prior to deposition. Therefore, at deposition, there is already a large number population of fine intermetallic particles in the droplets. Although some remelting, particularly of the smaller colder droplets in the spray, could be expected on deposition onto the growing billet surface, the billet surface temperature was always below the intermetallic reaction temperature so that the fine intermetallics formed initially in the droplets did not remelt entirely and disappear. Although these intermetallics could then coarsen in the residual billet liquid and subsequently in the solid state, in general, the coarsening was sluggish and a high number density of fine intermetallics was retained into the final billet. Overall, the heterogeneity in the local intermetallic particle population arose from the different thermal histories associated with the different sized droplets in the spray, which was not eradicated fully by remelting at deposition. In comparison with spray-formed conventional Al alloys that have a more homogeneous microstructure, the Al-Fe-Cr-Ti alloy had an unusually high fraction of thermally stable high-temperature IMCs, while the much higher melting temperature provided a stronger driving force for cooling that inhibited partial droplet/particle remelting at deposition, which is important in promoting microstructural homogeneity in spray forming.

Despite the extremely high 2θ resolution of ~0.005 deg at 10 keV of the I11 beamline at the Diamond Light Source, the high density of broadened, overlapping peaks in the XRD traces of the as-spray-formed microstructure precluded the use of standard ICDD cards for phase identification. Therefore, to determine the phases present, multiphase Pawley full pattern fitting from 3.5 to 50 deg 2θ (equivalent to ~6.5 to 104 deg 2θ for Cu $K_{\alpha 1}$ radiation) was performed. When Al, Al_3Ti (tetragonal), $Al_{13}Cr_2$, and $Al_{13}Fe_4$ were included in the refinement, a good fit to the experimental data was produced, as shown in Figure 3. However, there remained unmatched peaks at ~21.6 and 23.9 deg 2θ indicating the presence of a small fraction of an unidentified phase. For comparison, powder atomized Al-3Fe-2Cr-2Ti contained $Al_{13}(Cr,Fe)_{2-4}$ and/or $Al_{23}Ti_9$ as well as significant fractions of a nanoscale metastable icosahedral *i* phase.[7–9]

A small part of the billet was remelted fully and then gravity cast into a steel mold, followed by phase extraction and XRD. There were no unassigned peaks and $Al_{13}Cr_2$ and $Al_{13}Fe_4$ now dominated the phases. Therefore, despite the slower cooling rates of standard spray forming, it is suggested that a small fraction of an unidentified metastable phase(s) was retained into the final billet. However, transmission electron microscopy (TEM) studies were unable to identify any icosahedral (*i* phase) or other attributable phases beyond those

identified by synchrotron XRD. Although Al-3Fe-2Cr-2Ti has shown the capability to form *i* phase during rapid solidification,[7–9] there was no compelling evidence of as-spray-formed *i* phase, although the complexity of the microstructure and the potential for overlapping XRD peaks made it difficult to rule out conclusively the presence of *i* phase. The intermetallic particles identified after full remelting closely match those identified for solid-state mechanically alloyed Al-3Fe-2Cr-2Ti after heat treatment at 723 K to 773 K (450 °C to 500 °C).[11]

Figure 4(a) shows the bulk as-spray-formed synchrotron XRD trace for the range 2θ = 33 to 42 deg, together with the calculated position and shape of the α-Al peaks assuming only instrument broadening, *i.e.*, no stress or strain effects. The calculated peaks were much narrower than those obtained by experiment, suggesting a significant size and/or strain contribution to peak broadening. Figure 4(b) shows the same data with recalculated peaks in which broadening parameters due to both grain size and strain have now been adjusted to best fit the data. The fitting process yielded a crystallite size L_v, which is equivalent to D_V, the volume weighted domain size in Reference 17, and a residual strain. The fitting procedure was followed for various alloy conditions. At the as-spray-formed surface, the α-Al crystallite size was 210 nm, corresponding to a grain diameter of ~300 nm[17,18] and consistent with SEM imaging, recognizing that imaging estimates of grain size provide number-weighted data. TEM was also performed on thinned foils and measured grain sizes spanned 50 nm to 3 μm, with a predominance of grains of a few hundred nanometers. However, the synchrotron X-ray based measurements of grain size were held to be more representative of average grain sizes, since a much larger volume of material was sampled by the highly energetic X-rays than that imaged in TEM.

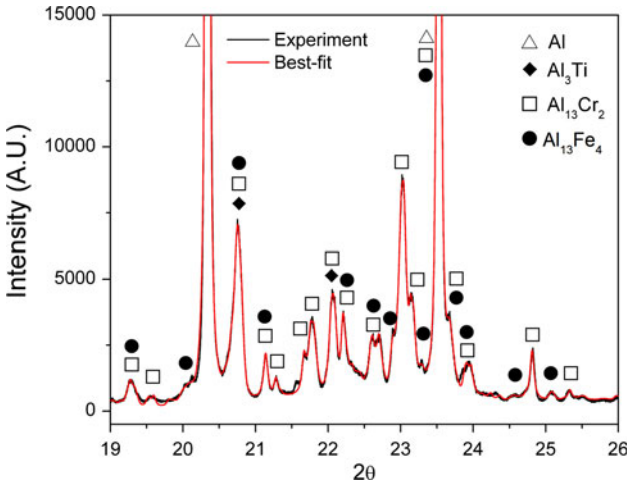

Fig. 3—Synchrotron XRD trace from the center of the as-spray-formed Al-2.7Fe-1.9Cr-1.8Ti billet and multiphase Pawley full pattern fitting indicating excellent agreement for the presence of α-Al, Al_3Ti (tetragonal), $Al_{13}Cr_2$, and $Al_{13}Fe_4$.

The as-spray-formed surface residual strain was 0.13, and there was a residual strain of 0.06 in the bulk for as-spray-formed, HIPed plus extruded, and HIPed plus forged conditions. Therefore, in all conditions at room temperature, there was considerable residual strain in the α-Al, arising from the very high fraction of intermetallic particles and differential thermal contraction during cooling.

B. *Consolidated Material*

Figure 5 shows backscattered electron images after HIPing at (a) 723 K (450 °C), 100 MPa for 4 hours and (b) 823 K (550 °C), 190 MPa for 2 hours. For both hot

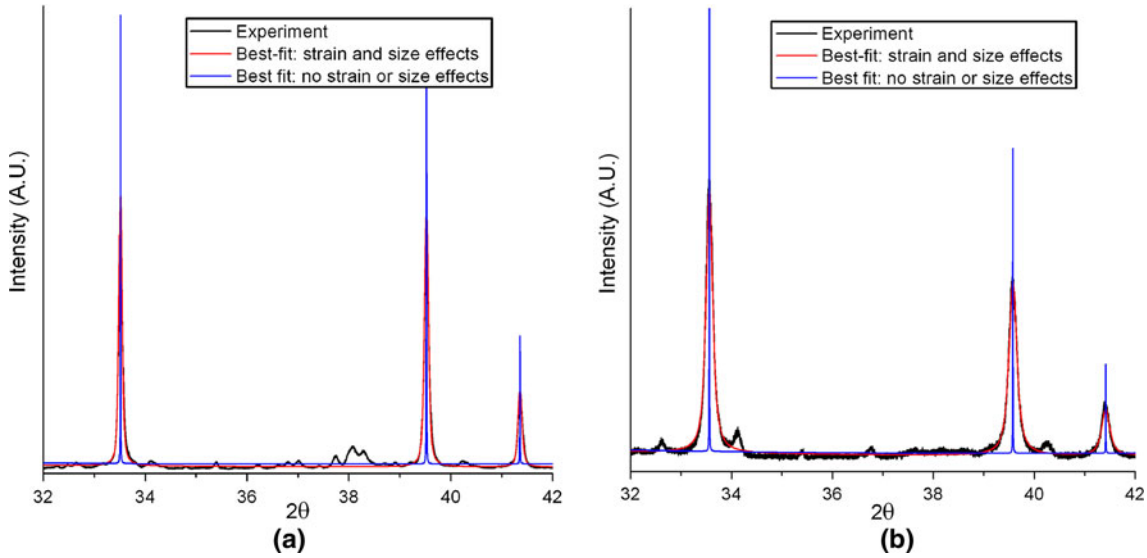

Fig. 4—(*a*) Experimental synchrotron XRD data and calculated Pawley fit to α-Al without crystallite size or strain effects in the 2θ = 33 to 42 deg range. (*b*) The same data allowing for crystallite size and strain, with the crystallite size and strain comprised of Lorentzian and Gaussian component convolutions varying in 2θ as a function of $1/\cos(\theta)$ and $\tan(\theta)$, respectively.

isostatic pressing (HIP) conditions, there was incomplete consolidation in local regions of very high volume fraction of nondeforming, hard intermetallic particles that prohibited diffusion bonding of the α-Al matrix. The heterogeneity in the microstructure persisted through the HIP cycle. HIP also formed Al-rich regions apparently absent in the as-sprayed condition, as shown arrowed in Figure 5, which increased in size and frequency with HIP temperature and pressure. These regions did not develop during heat treatment alone, and so the pressure of the HIP cycle must play a role in their formation. It is speculated that because of the inherent fine scale inhomogeneity of the sprayed microstructure, the strain associated with HIP will be concentrated in some regions of the microstructure. Strain concentrations may reduce the local thermodynamic stability of secondary phases and increase local diffusion rates by increasing defect density. Further studies are continuing into this phenomenon, but in the context of the current work, since the area fraction was <2 pct, they are assumed not to play a critical role in controlling bulk properties.

C. *Forging and Extrusion*

HIPed Al-2.7Fe-1.9Cr-1.8Ti was forged readily to a true strain of ~1 with no edge cracking. The material was also readily extruded at 16:1 at 748 K (475 °C) to an excellent surface finish. Figure 6(a) shows the extruded microstructure, including the Al-rich regions after HIP now drawn into elongated regions as indicated. After extrusion, no porosity could be detected by any method readily available. Figure 7(b) shows an electron backscattered diffraction (EBSD) map of the extruded structure with occasional larger, deformed α-Al grains denuded of intermetallics and containing retained subgrain structure associated with the deformation of the material by extrusion.

D. *Mechanical Properties*

Table I shows a summary of the room temperature tensile yield strength (YS), ultimate tensile strength (UTS), and elongation to failure of spray-formed Al-2.7Fe-1.9Cr-1.8Ti in various conditions, along with

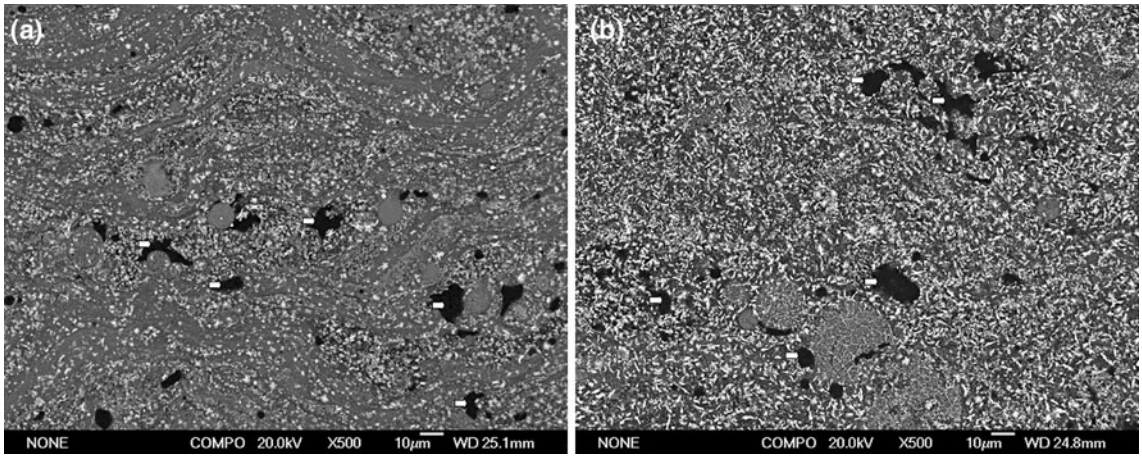

Fig. 5—Backscattered electron images of Al-2.7Fe-1.9Cr-1.8Ti HIPed at (*a*) 723 K (450 °C), 100 MPa for 4 h and (*b*) 823 K (550 °C), 190 MPa for 2 h. The black regions are Al-rich regions due to the relatively low atomic number of Al.

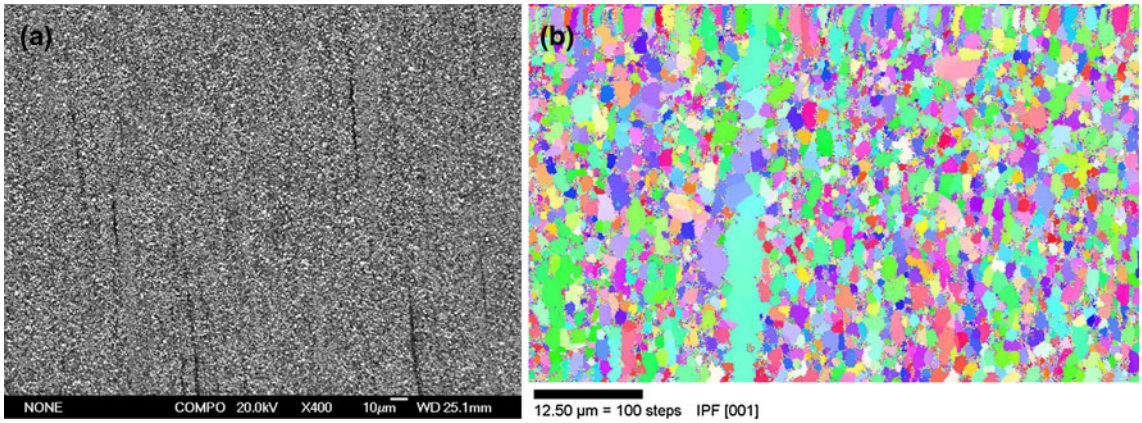

Fig. 6—(*a*) Spray-formed, HIPed, and extruded Al-2.7Fe-1.9Cr-1.8Ti and (*b*) EBSD orientation map showing occasional relatively large Al grains.

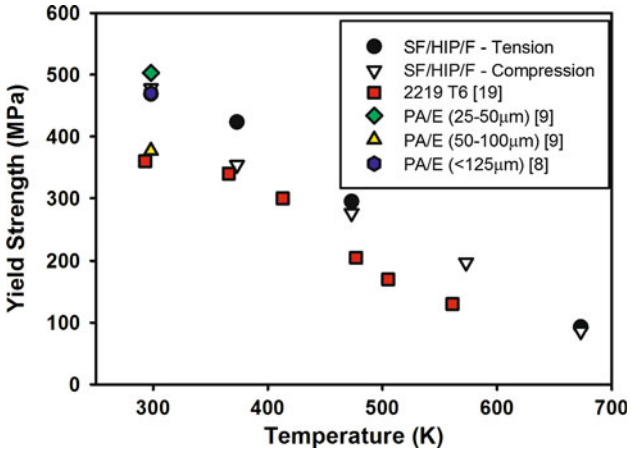

Fig. 7—YS of SF/HIP/F Al-2.7Fe-1.9Cr-1.8Ti, 2219-T6[19] and PA/E Al-3Fe-2Cr-2Ti using different powder diameters[8,9] as a function of temperature.

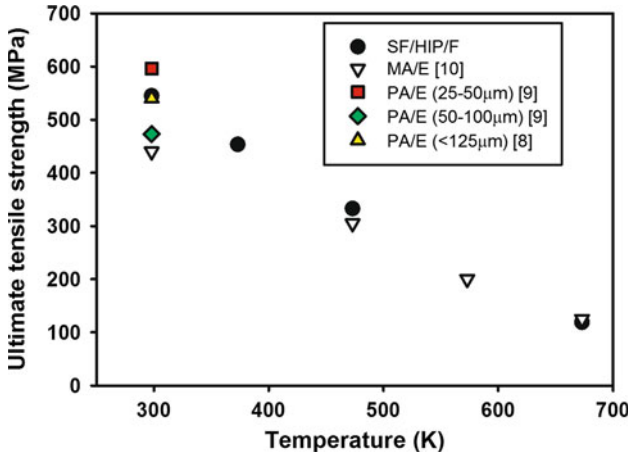

Fig. 8—UTS as a function of temperature for SF/HIP/F Al-2.7Fe-1.9Cr-1.8Ti and MA/E[10] and PA/E Al-3Fe-2Cr-2Ti.[8,9]

Table I. Tensile Properties at Room Temperature of Al-Fe-Cr-Ti Alloys Produced by Spray Forming and Powder Atomisation/Extrusion, in Various Conditions

Process condition	YS (MPa)	UTS (MPa)	Pct Elongation
SF/HIP 723 K (450 °C), 100 MPa, 4 h	418	548	2.6
SF/HIP 823 K (550 °C), 190 MPa, 2 h	253	389	4.8
SF/HIP/forged at 673 K (400 °C)	469	545	3.8
SF/HIP/extruded (16:1) at 748 K (475 °C)	371	463	6.8
Powder/extruded (25 to 50 μm)[9]	511	596	5.8
Powder/extruded (50 to 100 μm)[9]	378	474	7.5
Powder/extruded <26 μm[8]	550	660	~4.5
Powder/extruded <75 μm[8]	490	580	~3.3
Powder/extruded <125 μm[8]	470	540	~5.4

nominally Al-3Fe-2Cr-2Ti produced by alternative methods. HIP of the spray-formed billet at 823 K (550 °C) (SF/HIP) produced a relatively low YS and UTS due to excessive microstructural coarsening and a loss of solid solution strengthening due to excessive thermal exposure. HIP at the lower temperature of 723 K (450 °C), followed by forging at 673 K (400 °C) (SF/HIP/F), increased tensile performance to a YS = 469 MPa and UTS = 545 MPa, with a elongation to failure of 3.8 pct. Extrusion usually leads to additional texture strengthening in the extrusion direction, but in this case, an extrusion temperature of 748 K (475 °C) (SF/HIP/E) was too high to maintain microstructural stability (but was required so that the extrusion force was within the range of the extrusion machine) and resulted in a loss of strength. Even though the extruded room temperature strength was reduced, the extruded strength at elevated temperature was similar to that of the forged material and suggested that any residual porosity had a greater effect on undermining tensile strength at room/low temperature than at elevated temperature.

Spray forming, HIP, and forging (SF/HIP/F) provided properties significantly superior to suction casting (compressive YS = 232 MPa[6]) and similar to those obtained by powder atomization followed by extrusion. Only when the finest powder diameters produced by atomization were used did powder atomized and consolidated (and degassed) properties exceed those of spray-formed materials, because the higher cooling rates in these powders gave a significant fraction of the strengthening *i* phase.[7] However, the process yield of these powder diameters from atomization is generally low and consolidation restricted to limited geometries, whereas forging of larger spray-formed billets allows more flexibility in applications.

Figure 7 shows the tension and compression YS as a function of temperature for SF/HIP/F Al-2.7Fe-1.9Cr-1.8Ti, powder atomized/extruded (PA/E) Al-3Fe-2Cr-2Ti,[8,9] and high-temperature Al alloy 2219-T6.[19] The YS of SF/HP/F Al-2.7Fe-1.9Cr-1.8Ti was superior to that of high-temperature conventional Al alloy 2219 at all temperatures up to 673 K (400 °C). There was generally no significant tension/compression asymmetry on the SF/HIP/F alloy. Figure 8 compares the UTS of the SF/HIP/F Al-2.7Fe-1.9Cr-1.8Ti and mechanically alloyed/extruded (MA/E) Al-3Fe-2Cr-2Ti[10] as a function of temperature up to 673 K (400 °C) and the room temperature UTS of PA/E Al-3Fe-2Cr-2Ti. Again, the PA/E materials offered superior strength only when the finest powder diameters were selected, and the SF/HIP/F properties closely matched those of the MA/E route up to 673 K (400 °C). Figure 9 shows a typical room temperature fracture surface in the SF/H/F condition. There were a high number of dimples associated with the intermetallic particles. Subfailure surface cross-sectional microscopy showed failure was initiated by void nucleation around the intermetallic particles followed by both trans- and intergranular failure of the

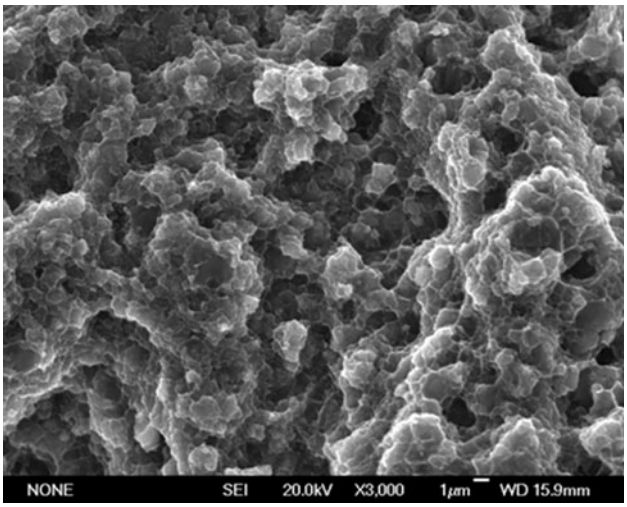

Fig. 9—Typical room temperature fracture surface in SF/H/F Al-2.7Fe-1.9Cr-1.8Ti showing failure initiated by void nucleation around intermetallic particles followed by trans- and intergranular failure of the fine scale α-Al matrix, with only limited plastic deformation.

surrounding fine scale α-Al grains, with only limited plastic deformation.

The spray-formed material had an α-Al grain size of at least 300 nm, whereas the MA/E material had a α-Al grain size of ~80 nm at room temperature, yet SF/HIP/F and MA/E properties were broadly similar. However, while the MA/E Al-3Fe-2Cr-2Ti was suggested to be essentially strain free at room temperature after extrusion and showed profound tensile-compression asymmetry,[10] there was significant residual strain in the SF/HIP/F alloy and there was no compression/tension asymmetry at any temperature up to 673 K (400 °C). The MA/E tension-compression asymmetry was ascribed to a dislocation-mediated plastic deformation mechanism that was intrinsic to the nanoscale grain microstructure and suggested to be intrinsic to Al-3Fe-2Cr-2Ti. However, based on the spray-formed materials examined here, extrinsic factors may need to be reconsidered, such as the role of oxides and carbides in the MA/E alloy,[20] while the spray-formed material is essentially free of carbides or oxides. The role of residual strain of up to 6 pct in the spray-formed material is likely to be complex, since the heterogeneous nature of the microstructure will lead to complex strain fields around the many intermetallic particles. Overall, it can be expected that these strain fields will interact with those due to dislocations and that residual strains make some contribution to strengthening. Finally, the criticality of obtaining *i* phase in this alloy in order to achieve desirable properties may need further consideration, since similar properties (at room temperature) have been obtained in the spray-formed material in bulk, without compelling evidence for the presence of a significant *i*-phase fraction. Consequently, the proposed mechanism of strengthening relying substantially on the unshearable nature of the *i* phase should be expanded to account for the role of other "conventional" intermetallic particles when present at a high fraction and the associated development of significant residual strain.

IV. CONCLUSIONS

Spray forming under standard conditions for conventional Al alloys has been investigated for a high-temperature Al-2.7Fe-1.9Cr-1.8Ti alloy previously studied by suction casting, powder atomization, and mechanical alloying. The as-spray-formed microstructure was inhomogeneous compared with conventional Al alloys, because the higher melting point gave a high driving force for melt cooling, and there was only limited remelting and flow on the billet top surface during manufacture. As-sprayed porosity was low at 2 to 3 pct and allowed standard downstream processes of HIP, forging, and extrusion to be applied. Although some minority phases could not be identified by XRD, there was no compelling evidence for the presence of significant metastable *i*-phase fractions. The microstructure contained a high volume fraction of hard intermetallic particles of micron and smaller size. X-ray synchrotron studies suggested an average α-Al grain size of ~300 nm and a residual strain of up to 6 pct in all conditions. Despite differences in phase content and microstructural scale, spray-formed, HIPed, and forged Al-2.7Fe-1.9Cr-1.8Ti showed broadly similar or superior tensile properties to very similar alloys produced by other routes. There was no tension/compression asymmetry and tensile properties were only exceeded by powder atomized/extruded equivalents when the smallest diameters were selected. Nonetheless, there remains a need to improve microstructural homogeneity and further optimize HIP and extrusion parameters. Overall, the conventional rapidly solidified microstructure and phases usually associated with Al-3Fe-2Cr-2Ti cannot be produced by spray forming under standard conditions. However, once downstream processing is considered, spray forming provided very similar properties to these materials, but in bulk and by forging, which together offer greater potential for scaleup to industrial applications.

ACKNOWLEDGMENTS

The authors thank the UK Engineering and Physical Science Research Council (Grant No. EP/E040608/1) for financial support and Dr. Julia Parker and Professor Chiu C. Tang for assistance at I11, Diamond Light Source. CB thanks the Royal Thai Government for financial support.

REFERENCES

1. C.R.M. Afonso, C. Bolfarini, C.S. Kiminami, N.D. Bassim, M.J. Kaufman, M.F. Amateau, T.J. Eden, and J.M. Galbraith: *Scripta Mater.*, 2001, vol. 44, pp. 1625–28.
2. C.R.M. Afonso, C. Bolfarini, C.S. Kiminami, N.D. Bassim, M.J. Kaufman, M.F. Amateau, T.J. Eden, and J.M. Galbraith: *J. Non-Crystalline Solids*, 2001, vol. 284, pp. 134–38.
3. M.-L. Ted Guo, C.Y.A. Tsao, J.C. Huang, and J.S.C. Jang: *Mater. Sci. Eng. A*, 2005, vol. 404, pp. 49–56.

4. M.-L. Ted Guo, C.Y.A. Tsao, J.C. Huang, and J.S.C. Jang: *Intermetallics*, 2006, vol. 14, pp. 1069–74.
5. M.-L. Ted Guo, C.Y.A. Tsao, K.F. Chang, J.C. Huang, and J.S.C. Jang: *Mater. Trans.*, 2007, vol. 48, pp. 1717–21.
6. V. Nagarajan: M. Met Thesis, University of Sheffield, Sheffield, United Kingdom, 2004.
7. M. Galano, F. Audebert, B. Cantor, and I.C. Stone: *Mater. Sci. Eng. A*, 2004, vols. 375–377, pp. 1206–09.
8. H.M. Kimura, K. Sasamori, and A. Inoue: *Mater. Sci. Eng. A*, 2000, vols. 294–296, pp. 168–72.
9. I. Todd, Z. Chlup, J.G. O'Dwyer, M. Lieblich, and A. García-Escorial: *Mater. Sci. Eng. A*, 2004, vols. 375–377, pp. 1235–38.
10. H. Luo, L. Shaw, L.C. Zhang, and D. Miracle: *Mater. Sci. Eng. A*, 2005, vol. 409, pp. 249–56.
11. L. Shaw, H. Luo, J. Villegas, and D. Miracle: *Acta Mater.*, 2003, vol. 51, pp. 2647–63.
12. L. Shaw, H. Luo, J. Villegas, and D. Miracle: *Scripta Mater.*, 2004, vol. 51, pp. 449–53.
13. C. Banjongprasert, S.C. Hogg, I.G. Palmer, and P.S. Grant: in *Proc. Solidification Processing 07*, H. Jones, ed., University of Sheffield, Sheffield, United Kingdom, 2007, pp. 636–40.
14. S.P. Thompson, J.E. Parker, J. Potter, T.P. Hill, A. Birt, T.M. Cobb, F. Yuan, and C.C. Tang: *Rev. Sci. Instrum.*, 2009, vol. 80, p. 075107.
15. R.A. Young: in *The Rietveld Method*, R.A. Young, ed., Oxford University Press, Oxford, United Kingdom, 1993, pp. 1–39.
16. P.S. Grant: *Metall. Mater. Trans. A*, 2007, vol. 38A, pp. 1520–29.
17. D. Balzar, N. Audebrand, M.R. Daymond, A. Fitch, A. Hewat, J.I. Langford, A. Le Bail, D. Louër, O. Masson, C.N. McCowan, N.C. Popa, P.W. Stephens, and B.H. Toby: *J. Appl. Cryst.*, 2004, vol. 37, pp. 911–24.
18. R. Delhez, T.H. de Keijser, J.I. Langford, D. Louer, E.J. Mittemeijer, and E.J. Sonneveld: in *The Rietveld Method*, R.A. Young, ed., Oxford University Press, Oxford, United Kingdom, 1993, pp. 132–66.
19. *ASM Metals Handbook*, vol. 2, *Properties and Selection: Nonferrous Alloys and Special-Purpose Materials*, 10th ed., ASM INTERNATIONAL, Materials Park, OH, 1990.
20. R.D. Schelleng, G.A.J. Hack, and J.H. Weber: *Proc. Conf. Advanced Al and Mg Alloys*, ASM INTERNATIONAL, Materials Park, OH, 1990, pp. 289–94.